

MERCURYDPM: FAST, FLEXIBLE PARTICLE SIMULATIONS IN COMPLEX GEOMETRIES PART B: APPLICATIONS

**Thomas Weinhart, Deepak R Tunuguntla, Marnix P van Schrojenstein Lantman,
Irana FC Denissen, Christopher R Windows-Yule, Harmen Polman,
Jonathan M F Tsang², Binbin Jin², Luca Orefice³, Kasper van der Vaart⁴,
Sudeshna Roy, Hao Shi, Arianna Pagano⁵, Wouter den Breeijen, Bert J Scheper,
Ahmed Jarray, Stefan Luding, Anthony R Thornton**

¹Multiscale Mechanics, Engineering Technology, MESA+, University of Twente
PO Box 217, 7500 AE Enschede, Netherlands

²DAMTP, Centre for Mathematical Sciences, University of Cambridge
Wilberforce Road, Cambridge, CB3 0WA, United Kingdom

³ Research Center Pharmaceutical Engineering GmbH,
Inffeldgasse 13, Graz, Austria

⁴Department of Civil and Environmental Engineering, Stanford University,
Stanford, CA 94305, USA

⁵Civil and Environmental Engineering, University of Strathclyde,
75 Montrose Street, Glasgow, G1 1XJ, United Kingdom

Key words: Granular Materials, DEM, *MercuryDPM*, Open-Source.

Abstract. *MercuryDPM* is a particle-simulation software developed open-source by a global network of researchers. It was designed *ab initio* to simulate realistic geometries and materials, thus it contains several unique features not found in any other particle simulation software. These features have been discussed in a companion paper published in the DEM7 conference proceedings; here we present several challenging setups implemented in *MercuryDPM*. Via these setups, we demonstrate the unique capability of the code to simulate and analyse highly complex geotechnical and industrial applications. The setups implemented include complex geometries such as (i) a screw conveyor, (ii) steady-state inflow conditions for chute flows, (iii) a confined conveyor belt to simulate a steady-state breaking wave, and (iii) a quasi-2D cylindrical slice to efficiently study shear flows. *MercuryDPM* is also parallel, which we showcase via a multi-million particle simulations of a rotating drum. We further demonstrate how to simulate complex particle interactions, including: (i) deformable, charged clay particles; and (ii) liquid bridges and liquid migration in wet particulates, (iii) non-spherical particles implemented via superquadrics. Finally, we show how to analyse and complex systems using the unique micro-macro mapping (coarse-graining) tool MercuryCG.

1 INTRODUCTION

MercuryDPM [1-3] is an open-source particle-simulation software written entirely in C++. Initially developed at the University of Twente, its developer/user community has grown rapidly, including researchers from the universities at Cambridge, Stanford, EPFL, Birmingham, Strathclyde, Sydney and Manchester. It was designed with the aim of allowing the simulation of realistic geometries and materials, found in industrial and geotechnical applications, and thus contains several unique features not found in any other particle simulation software: (i) a neighbourhood detection algorithm that can efficiently simulate *highly polydisperse packings*, which are common in industry [4]; (ii) an easy-to-use interface to define *complex walls*, making it easy to *exactly* model real industrial geometries [3]; and (iii) *MercuryCG* [5-8], a state-of-the-art analysis tool that extracts 3D continuum fields, providing accurate analytical/rheological information often not available from experiments or pilot plants. It further contains a *large range of contact models* to simulate complex interactions such as elasto-plastic deformation, sintering, breaking, wet and dry cohesion and liquid migration, all of which have important industrial applications. These features have been discussed in a companion paper published in the DEM7 conference proceedings [3]; here we present several challenging setups, implemented in *MercuryDPM*, that demonstrate those unique capabilities of the code.

2 COMPLEX GEOMETRIES

The following five applications demonstrate innovative geometries and boundary conditions that have recently been added to *MercuryDPM*.

2.1 Screw conveyor

Screw conveyors are mechanical devices ubiquitously used in the industry to transport material, generally in granular form. Despite its mechanical simplicity, the dynamics of the conveyed material inside of a screw feeder is complex, and strongly affected by the shape of the screw blade.

In most DEM solvers, the screw is implemented as a triangulated mesh: a collection of points on the screw surface is chosen and subdivided in triads, each of which will form a triangular tile covering the whole mapped surface. This way of implementing the surface of the screw, besides introducing artificial inaccuracies depending on the fineness of the mesh, can be problematic in the neighbourhood of sharp edges. In *MercuryDPM* both the helicoidal surface of a screw and a collision-detection algorithm between the screw and spherical particles is implemented analytically, which makes this approach more accurate and efficient.

The flow of a bi-disperse particle mixture inside a screw feeder is shown in Figure 2.1. The relative filling height (i.e. the height of the particle layer inside of the screw normalised by the screw diameter) is set to 0.35, while the screw rotates with an angular velocity of 2π rad/s. Figures a) and b) show that such devices trigger particle size segregation, due to both the shear between particles and screw components and the avalanching motion of the former. The rotation of the blade simultaneously lifts and pushes forward the particles, which are in a state of continuous avalanching, while the ones in contact with the external casing are greatly slowed by friction (see Figure 2.1c).

A better understanding of these complex dynamics might be useful for process optimization and design improvement, both of great importance in industrial processes. Applications of the model can range from pure DEM study of particle flow [22] to more complicated devices, such as roll compactors [23].

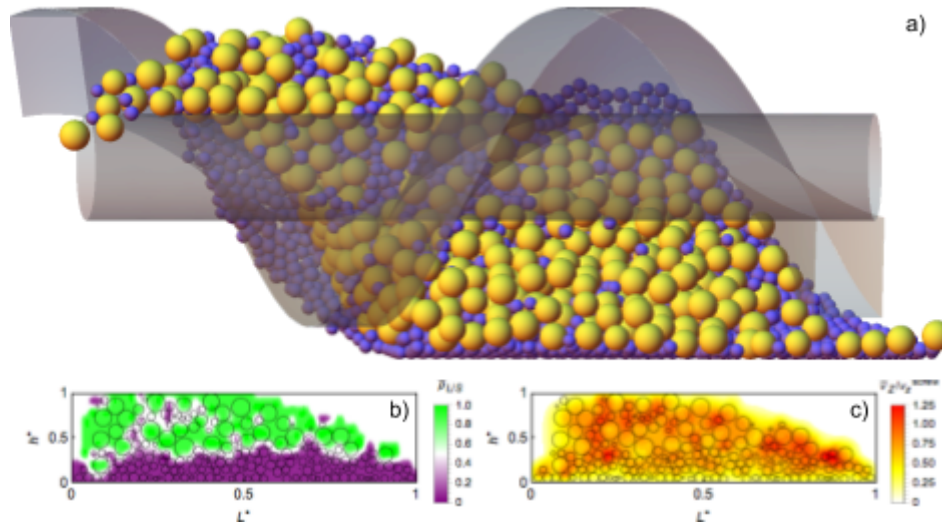


Figure 2.1 a) Snapshot of partially-filled screw feeder section transporting a bi-disperse particle mixture. Particles avalanche through the section, the screw surface being slightly shaded out for the sake of clarity. Particles coloured according to size. b) normalised coarse-grained density of big (green) and small particles (purple). The clear vertical separation shows particle size segregation. c) coarse-grained axial particle velocity normalized by screw axial velocity. The yellow particles in contact with the external casing are rotating with the screw, while particles in red are avalanching, triggering segregation.

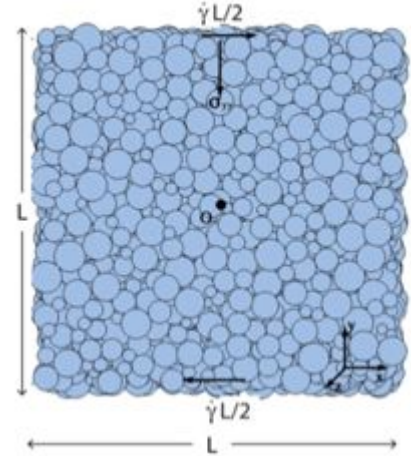
2.2 Pressure-controlled periodic walls.

To model granular materials on a macroscopic scale, rheological relations are needed that describe the response of the material (i.e. the changes in density and stress) to externally applied shear and compression. For each material, these relations can be measured experimentally, e.g. a direct shear box for soils or shear cells for powders. However, to study the effect of specific material properties on the rheological response, it is more insightful to use simulations rather than experiments, as parameters can be changed easily – and individually – allowing for reliable parameter studies. In addition, simulations allow us to set up ideal homogeneous conditions, which is not possible in experimental studies where one is constrained by the external boundaries of the experimental device.

Here, we present a simulation setup for measuring the material's response under controlled, homogeneous strain and pressure conditions, shown in Figure 2: A user-defined shear is enforced by applying Lees-Edwards boundary conditions, and a horizontal driving force is applied to the particles to enforce homogeneous shearing. To control the confining pressure, the boundaries as well as the particle bulk are compacting/dilating each time step according to a servo control. This setup allows user to explore two variables (shear rate and pressure) at the same time, with a low computational cost for each simulation. Figure 2 shows a polydispersed granular system (mean diameter d) containing 4096 soft particles. The initial

length of each side is $L=16d$. At the center point in xy -plane (marked as O), one always has zero mean field shear velocity during the whole simulation. The pressure σ_{yy} is kept constant along the y -direction, mimicking the confining pressure applied in experimental conditions. The servo-control is applied to dilate/compact the sample along the y -direction, which smoothly reaches its steady state. In order to investigate the sheared granular flow behavior with different inertia and particle stiffness, we systematically vary the both the confined normal stress σ_{yy} and shear strain-rate $\dot{\gamma}$ such that the dimensionless stress/softness $\sigma_{yy}(d/k_n)$ ranges between 10^{-3} and 10^{-1} and the dimensionless shear strain-rate $\dot{\gamma}(\rho_p d^3/k_n)^{1/2}$ is between 10^{-5} and 1.

Figure 2.2 Representative volume element (RVE) with 4096 polydispersed particles subjected to a constant shear rate and confining stress.



2.3 Head formation in bidispersed avalanche flows

In the simple setup of an inclined plane with particles glued to the surface, it is a known result that flow-particles of different sizes segregate; the larger particles move towards the free surface, while the smaller particles sink to the bottom. Because the flow-speed is higher near the free surface than at the bottom, the large particles are transported towards the front. This leads to a flow front consisting of large particles, with a higher basal friction than the rest of the flow. This causes the front to be slower than the flow coming from behind, resulting in a bulbous head [14]. This bulbous head is much longer than it is high, so one needs many particles in order to be able to observe it in discrete particle simulations [15].

To implement this setup efficiently, we designed a Maser inflow boundary that produces a steady flow of particles, shown in Figure 2.3. The Maser boundary splits the domain into two parts: a small periodic chute with a steady flow, and the actual, much longer chute. Initially, the periodic chute runs until it reaches a steady state in both the flow- and segregation profile. Then, the Maser boundary is allowed to produce particles in the outflow domain: every particle in the periodic domain that crosses the downslope periodic boundary is both transported to the upslope boundary *and* copied into the outflow domain. One of the main advantages of this mechanism is that particles are only generated when needed: there is only a small number of ‘extra’ particles that need to be simulated at any given time, and one does not need to estimate the total number of particles in advance. The second advantage is that the Maser boundary generates a flow that is uniform and steady at the inflow; this reduces the distance in the flow has to travel before a steady bulbous head develops. Often a significant proportion of the simulation time goes into the inflow hopper or chute; the Maser removes the need to accurately simulate the inflow apparatus leading to a significant improvement in performance. In the future, we wish to use the Maser inflow boundary to generate data sets for full-scale chute flows, to investigate the use of flows over small periodic chutes and moving-bed channels as models for the full-scale chute flows.

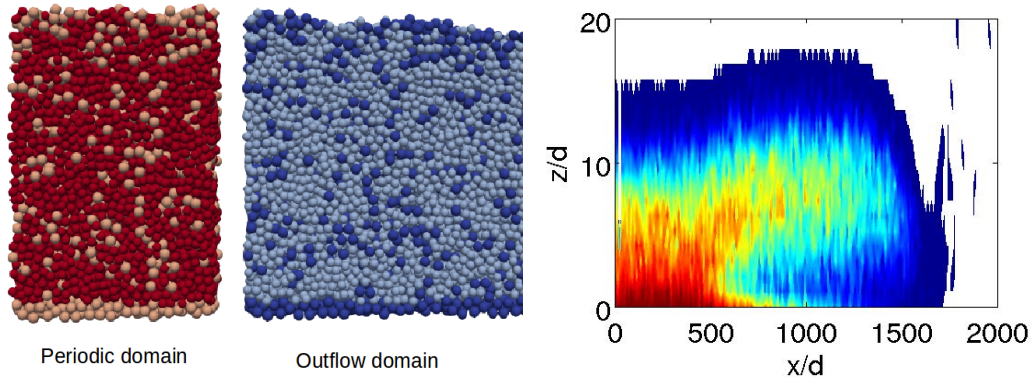


Figure 2.3: (a) Maser inflow boundary: the steady flow in the periodic domain generates particles for the full-scale chute flow in the outflow domain. Every time that a particle crosses the periodic boundary on the righthand side, it is simultaneously moved to the periodic boundary on the lefthand side and also copied in the outflow domain. (b) Bulbous head in shallow bidisperse chute flow. The colour-bar refers to the small-particle concentration: red is mostly small particles, blue is mostly large particles.

2.4 Breaking size-segregation waves in a moving-bed channel

As discussed in the previous section, size-segregation in a gravity-driven free-surface flow typically gives rise to the formation of a large-particle rich front and a small-particle rich tail. Separating these two regions is a recirculating structure where large particles, which have been deposited on the bed and overrun by the advancing flow front, are re-segregated to the free surface. At the same time small particles segregate to the bed in this region. This recirculating structure is referred to as a *breaking size-segregation (BSS) wave* [9, 10].

Simulating a BSS wave is challenging because of its time-dependent nature. BSS waves develop slowly, and after one has formed it travels close to the front of the flow. However, the BSS wave often travels slower than the front: as more large particles are carried to the front than are deposited on the bed, the large-particle front grows, thereby pushing the BSS wave back [11]. Thus, in order to study BSS waves in simulations, a very long chute is required to allow a steady BSS wave to emerge, and even then the BSS wave will be difficult to track. An alternate option is the use of a moving-bed channel [12,13]. In a moving-bed channel the bed is not rigid but consists of a moving conveyor belt that drags bottom layers of the flow upslope. At the same time the upper layers of the flow will still avalanche downslope. This creates a steady flow that remains stationary in the reference lab frame. A large-particle front and small-particle tail can develop in this flow configuration and thus also a BSS wave. Due to the compact setup of the moving-bed channel, the BSS wave reaches a steady-state position in a relatively short computational time. The particle positions, forces and velocities can then be time-averaged and coarse-grained for analysis.

Figure 2.4(a) shows a snapshot of a simulation of a bidisperse mixture of grains in a moving-bed channel. Large particles have accumulated at the downslope end of the channel (high x) while small particles have accumulated at the upslope end of the channel (low x). In between the tail and front exists a mixed region which is the BSS wave. Figure 2.4(b) shows a time- and width-averaged coarse grained field of the local small particle volume fraction ϕ_s . Here the structure of the BSS wave is more clearly visible. Note that ϕ_s is defined such that the small and large particle volume fraction sum to unity: $\phi_s + \phi_l = 1$.

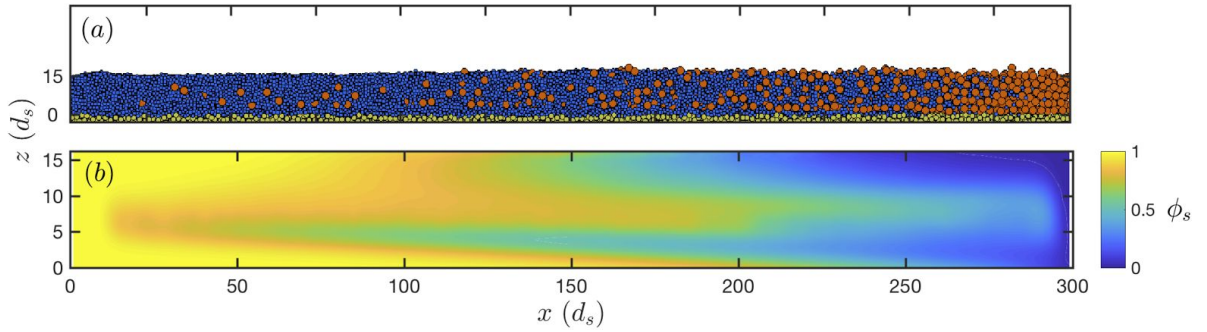


Figure 2.4: (a) Bidisperse granular mixture ($d_l/d_s=2.4$) in moving-bed channel geometry. The channel is inclined such that the mixture flows in x -direction. At the same time, the channel bed (yellow) moves in negative x -direction, dragging bottom layers of the flow upslope. This creates a steady granular flow. Size-segregation causes a large-particle rich front and a small-particle rich tail, separated by a breaking size-segregation wave. (b) Time- and width-averaged coarse-grained small-particle volume fraction.

2.5 Fingering instability in bidispersed avalanche flows

Under suitable circumstances, an avalanche of a bidisperse granular mixture is unstable to the *fingering instability* [16]. The avalanche is initially homogeneous in the cross-slope direction, but its front breaks into fingers, and the resulting flow has a longer runout distance than that of monodisperse avalanches of each separate species.

This instability is driven by granular segregation. For example, suppose the two species have different sizes but the same density. Segregation drives the larger species to the top of the avalanche. Being at the top, this species travels faster and ends up at the front of the avalanche. If the larger species is also more frictional, then this part of the front moves more slowly than the region of the avalanche behind it; consequently, the avalanche pushes through the front. For the instability to occur, the segregation should act quickly, and the larger species should be much more frictional than the smaller one, so that the front may become very slow.

We successfully realised examples of the fingering instability using *MercuryDPM*. We found that sliding friction does not sufficiently slow the motion of the larger species, even if the friction coefficient is increased to unphysically high levels. Laboratory experiments suggest that the friction of the larger species comes from the particles' angularity instead of an intrinsic friction of their material. This angularity can be captured in a simulation of spherical particles by introducing a rolling resistance.

Future work will involve systematic comparisons of these simulations against laboratory experiments and continuum models. In particular, as the 'coefficient of rolling friction' in the Iwashita–Oda model [17] does not correspond to a physical quantity, it must be calibrated by looking at its effects on bulk friction angles.

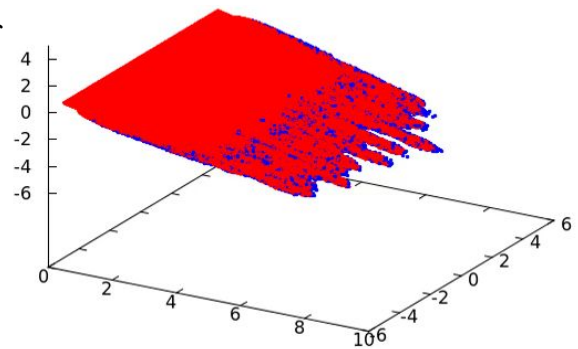


Figure 2.5 Example of granular fingering in *MercuryDPM*. The blue particles are approximately twice the diameter of the red particles, and have higher coefficients of sliding and rolling friction.

3 FULLY PARALLELISED LARGE-SCALE SIMULATIONS

To enable large scale simulations, *MercuryDPM* is MPI-parallelised, which we showcase via a multi-million particle simulation of a long rotating drum.

3.1 Long rotating drums

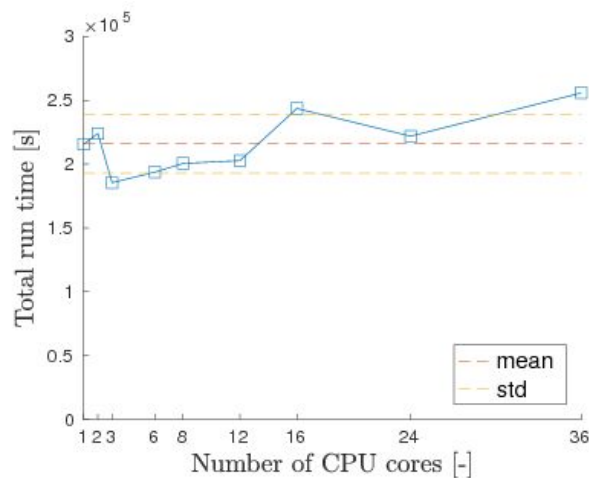
Rotating drums or tumblers are widely used in a range of industrial sectors to process granular and particulate media. One of the most common applications of the rotating drum geometry is the mixing of two or more physically dissimilar ‘species’ of particulate. In granular systems as a whole, dissimilar particle species are prone to segregate when exposed to external excitation. In the rotating drum geometry, this can manifest itself as either *radial segregation* (whereby one species will segregate towards the radial centre of the system) or *axial segregation* (whereby the system will segregate along its axial length into distinct ‘bands’ of differing species).

While radial segregation can be observed in systems of almost any aspect ratio, axial segregation is typically observed to manifest itself only in systems with relatively great axial lengths. Simulating long drums is challenging, as a longer system will contain a greater number of particles and thus be significantly more computationally expensive to simulate.

The fully-parallelised nature of *MercuryDPM* means that, with access to an adequately large number of processors, it is possible to efficiently simulate systems of arbitrary length, and thus to gain valuable insight into the axial banding phenomenon, and indeed other behaviours which may only become significant in drums possessing large aspect ratios.

In Figure 3.1 we demonstrate the extent to which *MercuryDPM*’s parallel processing capability can expedite large simulations. By increasing the number of processors used by the code in proportion to the length of the drum (and hence the number of particles within the system), it is possible to maintain a near-constant simulation time, as opposed to the linearly increasing time required for a non-parallelised code. In other words, we can simulate systems containing of the order of 1,000 particles within a similar timeframe to a system containing many hundreds of thousands of particles.

Figure 3.1. Computational run time required for 2.4 million timesteps of the rotating drum simulation. The number of particles per core is kept constant while increasing the number of cores. The computational cost is nearly constant, showing good parallel scalability.



4 COMPLEX PARTICLE AND CONTACT PROPERTIES

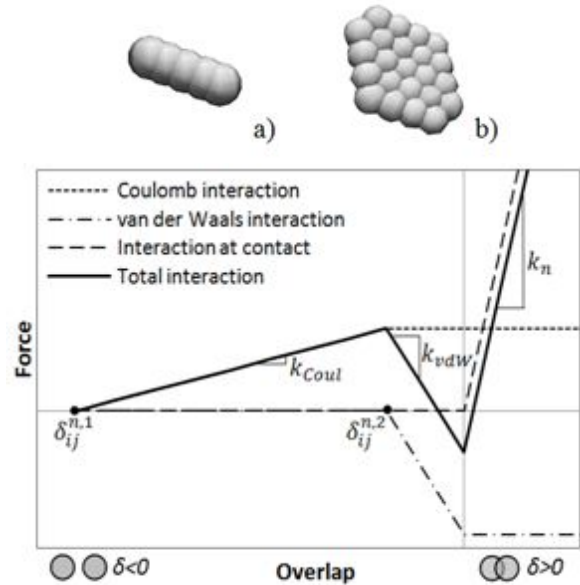
4.1 Modelling clay

Simulating clayey geomaterials using DPM is a great challenge, with many issues remaining to be solved. Firstly, physico-chemical microscopic interactions between particles have to be taken into account, as well as conventional mechanical interactions. Such interactions, mainly attributed to Coulomb repulsion/attraction and van der Waals forces, affect particles arrangement and are known to control the macroscopic behaviour of clays. On the other hand, the plate-like (3D) or rod-like (2D) shape of clay particles plays a key role in the interpretation of soil macroscopic behaviour and cannot be ignored during the analysis.

A modified contact model for simulating clayey geomaterials was implemented using *MercuryDPM* [20]. The first interaction is the conventional relationship between the overlap of particles in contact, δ_{ij} , and the repulsive contact force in the normal direction, f_{ij} , developing when overlapping occurs ($\delta_{ij} > 0$). The second interaction has to be defined as the relationship between the particles distance ($\delta_{ij} < 0$) and the attractive/repulsive force developing before the overlap occurs. These ‘long range’ forces are able to mimic the effect of Coulomb interactions, either repulsive or attractive, and van der Waals interaction, generally assumed to be attractive for clay particles. The total force acting on the particles is obtained by adding these three contributions together. A qualitative example of the implemented contact model is shown in Figure 4.1a.

Both rod-like and plate-like particles have been implemented, shown in Figure 4.1a/b. In addition to the previously mentioned contact law, an additional attractive interaction has been added that glues together particles belonging to the same rod or platelet.

Figure 4.1 a) rod-like and b) plate-like particle shapes. c) Qualitative example of implemented contact model



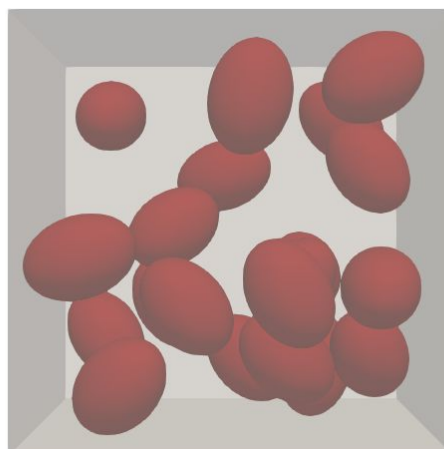
4.2 Non-spherical particles

Besides utilising the multi-sphere approach shown in Sec. 4.1, *MercuryDPM* supports convex-shaped, superquadric particles, whose shape is described by the following equation:

$$f(x, y, z) = \left(\left| \frac{x}{a} \right|^{n_2} + \left| \frac{y}{b} \right|^{n_2} \right)^{n_1/n_2} + \left| \frac{z}{c} \right|^{n_1} - 1 = 0.$$

Note that (n_1, n_2, a, b, c) are the parameters defining the superquadric. For example, we get a cuboid with rounded-edges when $n_1 \gg 2, n_2 \gg 2$ and $a \neq b \neq c$. Other shapes can be defined similarly by changing the values of the exponents (blockiness parameters) and the axis-scales (half-lengths). As a result, it is now possible to have ellipsoids and rounded cubes in the same simulation. Hence, enabling simulations of complex realistic granular phenomena.

Figure 4.2: Example of free cooling of elliptical particles in a box. Ellipsoids are given an initial position and velocity and interact with each other and the side-walls.



4.3 Wet particles in a cylindrical shear cell

This simulation combines complex boundary conditions (a pie-shaped periodic boundary and moving walls) with a complex contact law (adhesive liquid bridge forces and liquid migration). Cylindrical shear cells are often used as rheometers as they allow the application of continuous shear. However, simulating a whole cell is expensive because of the large amount of particles involved. We therefore use the symmetry in angular direction and simulate only a slice, shown in Figure 4.3. For this, a special angular periodic boundary has been developed [18,19]. We use a phenomenological contact model combining an elastic repulsive force and a hysteretic liquid bridge capillary force based on the particle specifications, contact properties and liquid properties/ saturation in the system [19].

In our initial simulations, a simplistic situation is assumed where all contacts have liquid bridges of equal volume. In this case, the liquid in the system is not treated as a separate entity, rather the contact model takes accounts for the mean effect of liquid capillary bridges.

We then extended this model to account for liquid migration. The methodology is quite straight forward: liquid is transferred locally whenever contacts are formed or broken. Thus, the particles and the liquid are considered as two different entities in the system. Liquid is either associated with the particles as a thin liquid film, or with the contacts as liquid bridges. Film volumes are free to form new liquid bridges, whenever contacts are formed. Unlike film volumes, bridge volumes are bound to contacts till they are ruptured. When a liquid bridge is ruptured, bridge volumes are distributed neighbouring contacts and particles, as demonstrated in Figure 4.3. Total liquid conservation is ensured. The microscopic simulations of liquid migration allow the validation of a continuum scale model that describes the migration of liquid as shear-rate dependent diffusion.

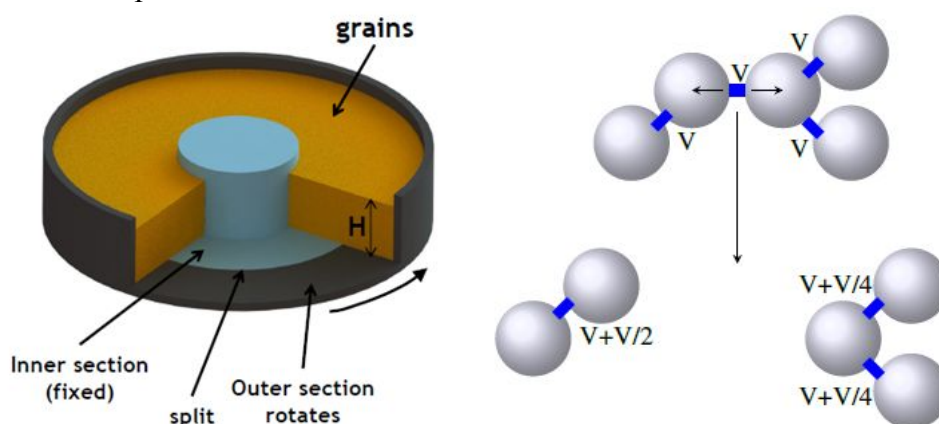


Figure 4.3 (a) Split bottom shear cell set-up (b) Bridge rupture according to liquid migration scheme [21]

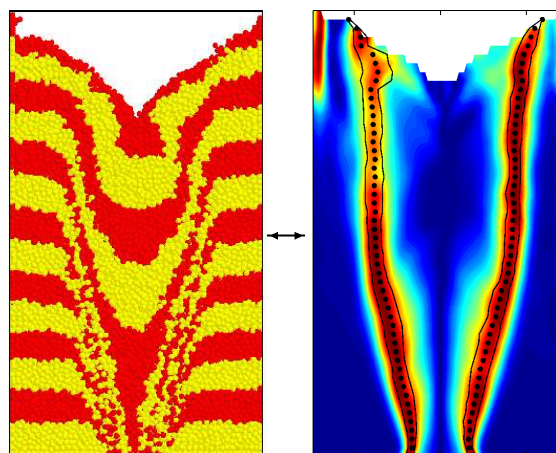
5 COARSE-GRAINING ANALYSIS

In this final section, we demonstrate the capabilities of *MercuryCG*, our state-of-the-art analysis tool that extracts 3D continuum fields from particle simulations and experiments.

5.1 Silo Flow

The coarse-graining method implemented in *MercuryCG* [5-8] allows the calculation of continuum quantities (density, velocity, stress, and many more), even in regions with large spatial or temporal gradients. These measurements can then be used to characterise the macroscopic material properties (i.e. their rheology) and develop continuum models that describe the bulk behaviour. In [8], a silo flow model with a complex internal flow pattern was studied as a test case, where all three dense flow regimes are present, i.e.: (i) a stagnant zone, (ii) a highly localised shear band and (iii) a core zone with fast flow. The coarse-graining method was not only able to determine those zones (see Figure 8), but was further used to show the differences in rheological properties of the materials in each zone. This innovative use of continuum fields in the analysis of particle data may extend the range of validity of current rheological models, increasing their predictive capability.

Figure 5.1: Silo flow in a quasi-2D geometry (left). The coarse-grained shear rate (right) can be used to distinguish three flow regimes: (i) a stagnant outer zone, (ii) a highly localised shear zone, and (iii) a fast-flowing core zone.



5.2 Experimental coarse-graining

Another key technology in the quest for characterisation of particles flow and dynamics is the particle tracking techniques. A particle tracking tool is being developed to convert data from experiments into data which can be read and post-processed by the coarse-graining method implemented in *MercuryCG*. This allows researchers and engineers to obtain quantitative and qualitative visualisation of the velocity gradient and distribution of particles. It can also be used to export multiple parameters of the particles flow. The tool is currently capable of tracking and processing optical data and Positron Emission Particle Tracking data (PEPT). In our development of this Tracking-MercuryCG tool, we aspire to extend its capability to track RIMS and NMRI data.

In Figure 5.2, we show a snapshot of a rotating drum filled with glass beads that rotates at 25 rpm. The flow of particles in this apparatus is an example of experimental data that can be processed using the Tracking-MercuryCG tool. In this case, slow motion video of a rotating drum is recorded using a MotionBLITZ EoSens high speed camera working at a speed of 460 frame/s (Figure 5.2 left). The video is then post-processed using the tracking tool where the dark glass beads in the drum are detected and tracked. Velocity gradient are afterward

generated using *MercuryCG*. In Figure 5.2 right, a coarse-grained velocity gradient of this experimental data is shown for dry and wet glass beads. In the upper part of the bed, the hot colours indicate areas where the local velocity of the particles is high, while cooler colours in the core of the bed indicate regions where the velocity of the glass beads is lower.

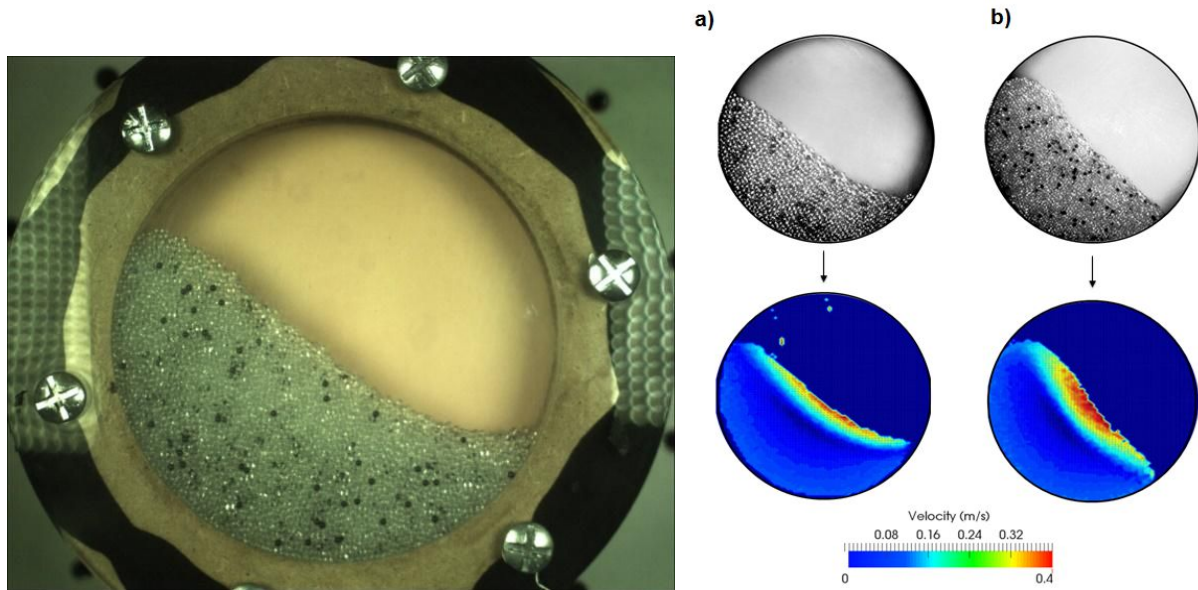


Figure 5.2 Left: Rotating drum apparatus: example for post-processing experimental data, using the particles tracking tool and coarse-graining. Right: Coarse-grained velocity gradient of the rotating drum at 25 rpm. a) Dry glass beads, b) Wet glass beads.

6 CONCLUSIONS

MercuryDPM is an open-source software based on a flexible, object-oriented framework, making it easy for users to customise the geometry and material properties to an extent not available in traditional particle simulation software. This has led to several innovative features such as complex in- and outflow conditions, curved walls, and pressure-controlled periodic walls. As the code is developed as an open-source project, users can merge their newly developed features into the publicly-available software, making it available to all *MercuryDPM* users. The codes presented here are available, or will be made available shortly, in the public *MercuryDPM* release, available at MercuryDPM.org; previews of the unreleased code are available in the current *MercuryDPM*-Alpha, which is available on request. A description of the files needed to run a specific application can be found at <http://MercuryDPM.org/Documentation/Applications>. We welcome you to use these features, give us feedback, and even become a developer should you choose to give back features to the *MercuryDPM* community. Just contact us via info@mercurydpm.org.

ACKNOWLEDGEMENTS

We acknowledge the support of the following grants: NWO VICI 10828; NWO VIDI 13472; STW 11039; STW-DFG 12272; DFG SPP1482 B12; DFG LU 450/10.

REFERENCES

- [1] Thornton, A.R., Krijgsman, D., te Voortwis, A., Ogarko, V., Luding, S., Fransen, R., Gonzalez, S. I., Bokhove, O., Imole, O. and Weinhart, T., A review of recent work on the Discrete Particle Method at the University of Twente: An introduction to the open-source package MercuryDPM, *Proc. 6th International Conference on Discrete Element Methods* (2013).
- [2] Thornton, A.R., Krijgsman, D., Fransen, R., Gonzalez, S., Tunuguntla, D. R., ten Voortwis, A., Luding, S., Bokhove, O. and Weinhart, T., Mercury-DPM: Fast particle simulations in complex geometries, *EnginSoft Year 10(1)* (2013).
- [3] Weinhart, T., Tunuguntla, D. R., van Schrojenstein Lantman, M., van der Horn, A. J., Denissen, I. F. C., Windows-Yule, C. R. K., de Jong, A. C. and Thornton, A. R., MercuryDPM: A fast and flexible particle solver Part A: Technical Advances, *Proc. 7th International Conference on Discrete Element Methods* (2016).
- [4] Krijgsman, D., Ogarko, V. and Luding, S., Optimal parameters for a hierarchical grid data structure for contact detection in arbitrarily polydisperse particle systems, *Comp. Part. Mech. 1(3)*, (2014).
- [5] Weinhart, T., Thornton, A.R., Luding, S. and Bokhove, O., From discrete particles to continuum fields near a boundary, *Granul. Matt. 14(2)*, 289-294 (2012).
- [6] Tunuguntla, D. R., Thornton, A. R. and Weinhart, T., From discrete particles to continuum fields: Extension to bidisperse mixtures. *Comp. Part. Mech. 3(3)*, 349-365 (2016).
- [7] Weinhart, T., Hartkamp, R., Thornton, A.R. and Luding, S., Coarse-grained local and objective continuum description of 3D granular flows down an inclined surface, *Phys. Fluids 25*, 070605 (2013).
- [8] Weinhart, T., Labra, C., Luding, S. and Ooi, J., Influence of coarse-graining parameters on the analysis of DEM simulation results, *Powder Technol. 293*, 138-148 (2016). *Preprint*
- [9] Thornton, A. R. and Gray, J. M. N. T., Breaking size segregation waves and particle recirculation in granular avalanches, *J. Fluid Mech. 596*, 261–284 (2008).
- [10] Gajjar, P., van der Vaart, K., Thornton, A. R., Johnson, C. G., Ancy, C. and Gray, J. M. N. T., Asymmetric breaking size-segregation waves in dense granular free-surface flows, *J. Fluid Mech.*, 794, 460–505 (2016).
- [11] Gray, J. M. N. T. and Kokelaar, B. P., Large particle segregation, transport and accumulation in granular free-surface flows, *J. Fluid Mech. 652*, 105–137 (2010).
- [12] Davies, T. R. H., Debris-flow surges - experimental simulation, *J. Hydrology 29(1)*, 18–46 (1990).
- [13] Chambon, G., Ghemmour, A. and Laigle, D., Gravity-driven surges of a viscoplastic fluid: An experimental study, *J. Non-Newtonian Fluid Mech. 158(1)*, 54–62 (2009).
- [14] Kokelaar, B.P., Graham, R.L., Gray, J.M.N.T. and Vallance, J.W., Fine-grained linings of leveed channels facilitate runout of granular flows, *Earth and Planetary Sci. Lett. 385*, 172-180 (2014).
- [15] Denissen, I. F. C., Weinhart, T., te Voortwis, A., Luding, S., Gray, J. M. N. T. and Thornton, A.R., Bulbous head formation in bidisperse shallow granular flow over an inclined plane. *J Fluid Mech.* (2017). *Under Review*
- [16] Pouliquen, O. and Savage, S. B., Fingering in granular flows. *Nature 386* (1997).
- [17] O’Sullivan, C. *Particulate Discrete Element Modelling: A Geomechanics Perspective*, CRC Press (2011).
- [18] Roy, S., Luding, S. and Weinhart, T., A general(ized) local rheology for wet granular materials, *New J. Phys. 19*, 043014 (2017).
- [19] Roy, S., Singh, A., Luding, S. and Weinhart, T., Micro-macro transition and simplified contact models for wet granular materials, *Comp. Part. Mech. 3(4)*, 449–462 (2016).
- [20] Pagano, A. G., Tarantino, A., Pedrotti, M., Magnanimo, V., Windows-Yule, C. R. K. and Weinhart, T. Micromechanics of non-active clays in saturated state and DEM modelling, *Proc. 8th International Conference on Micromechanics of Granular Media* (2017).
- [21] This figure is taken from the presentation of Dr. Ken Kamrin, which was given at the KITP Conference on Complexity in Mechanics (2014), http://online.kitp.ucsb.edu/online/nonequil_c14/kamrin/
- [22] Orefice, L. and Khinast J.G., DEM study of granular transport in partially filled horizontal screw conveyors, *Powder Technol. 305*, 340-346 (2017).
- [23] Mazar, A., Orefice, L., Michrafy, A., de Ryck, A. and Khinast, J.G., A combined DEM & FEM approach for modelling roll compaction process, *Powder Technol.* (2017). *In press*